Optical Resonators With Variable Reflectivity Mirrors

By H. ZUCKER

(Manuscript received May 27, 1970)

In this paper we investigate circular optical resonators with gaussian profiles of the mirror reflectivities. Closed form solution to the integral equations for such resonators are obtained. The dominant $TEM_{0,0}$ mode characteristics of a resonator consisting of one variable reflectivity mirror (VRM) and one uniform reflectivity mirror (URM) are considered in detail for a variety of parameters. This resonator is particularly suitable for high-gain lasers. Its advantages in comparison to the conventional type are: (i) there is larger mode volume utilization, and (ii) the power transmitted at the variable reflectivity mirror can in principle be utilized as the power output. We discuss dependence of the spot sizes on laser gain and mirror-curvature tolerances and present a specific design of a Fabry-Perot resonator for fundamental mode operation and the expected performance.

I. INTRODUCTION

The dominance of the fundamental mode in optical resonators with uniform reflectivity mirrors is due to the lowest diffraction loss of this mode. The power output of this mode is commonly obtained by using a partially transparent mirror. These two features could be combined in a resonator consisting of one uniform reflectivity mirror (URM) and one variable reflectivity mirror (VRM).

Resonators with VRM were investigated previously. S. N. Vlasov and V. I. Talanov[1] considered symmetrical two-dimensional resonators with two types of variations of the mirror reflectivities including the gaussian and obtained solutions for the eigenvalues of the resonator integral equations. N. G. Vakhimov[2] investigated the natural resonant frequencies and field distributions of symmetrical resonators with gaussian VRM by using an asymptotic method of solution to the wave equation subject to impedance boundary conditions. N. Kumagai and others[3] investigated Fabry Perot resonators with VRM of finite dimen-

sions by solving numerically the resonator integral equation for different mirror reflectivities. Y. Suematsu and others[4] studied beam waveguides with gaussian transmission filters for the improvement of the stability of beam transmission.

In this work we investigate nonsymmetrical circular resonators consisting of one URM and one VRM. The radii of curvature of the mirrors are arbitrary. The reflection coefficients of the VRM are assumed to have gaussian profiles in the radial direction. For such resonators with infinite mirrors, solutions to the resonator integral equations are obtained in terms of Laguerre functions with complex arguments. The modal fields decrease off-axis very rapidly and consequently these solutions are also applicable to resonators with finite mirrors.

Resonators of the type considered seem to be particularly suitable for high-gain lasers as for example CO_2 lasers. It is shown subsequently that for the fundamental $TE_{0,0}$ mode, the spot sizes obtainable are considerably larger than those obtained with URM resonators of the same length and the same fundamental mode threshold gain ratio. This should result in a larger mode volume utilization. Furthermore, the power loss due to the transparency of VRM could be utilized as the power output.

In the following sections the solutions for the resonator modes and eigenvalues of nonsymmetrical resonators are obtained. It is shown that the solutions for symmetrical resonators consisting of two identical VRM are readily obtainable as special cases. Mode-stability criteria are established as functions of the resonator geometries and VRM parameters. The spot sizes of the fundamental $TE_{0,0}$ mode are computed as a function of the threshold-gain ratio for a variety of parameters. A comparison is made between the obtainable spot sizes with Fabry Perot resonators with VRM and URM. We show that much larger spot sizes can be achieved with the VRM resonator. We show also that the spot-size diameters of VRM mirrors depends basically on the threshold-gain ratio and on the mirror-curvature tolerances. A specific design of a Fabry Perot resonator with a VRM is examined and the expected performance is presented.

II. NONSYMMETRICAL RESONATORS

2.1 *Solutions to the Integral Equation (IE)*

The geometry of the nonsymmetrical resonator is shown in Fig. 1. It consists of one mirror with variable reflectivity (M1) and one mirror

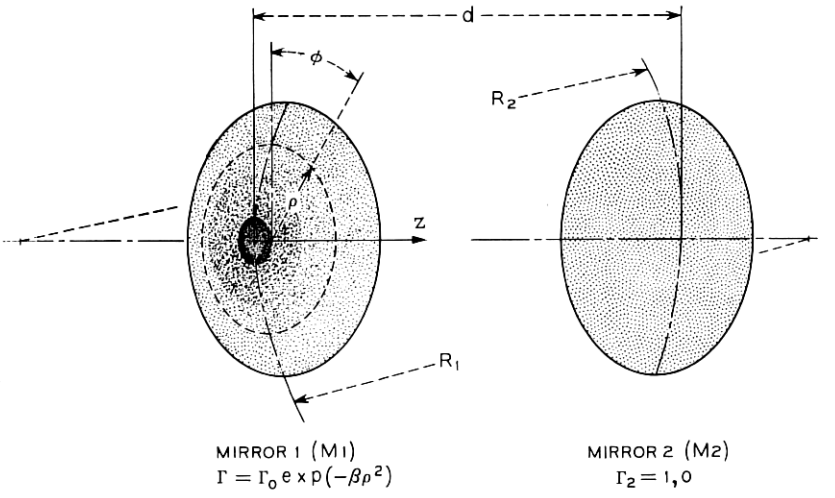

Fig. 1—Nonsymmetrical resonator.

with uniform reflectivity (M2). The separation between the mirrors is d, and the radii of curvature are designated by R_1 and R_2 respectively. The reflection coefficients of the VRM, Γ, is assumed to vary in the radial direction ρ as follows:

$$\Gamma = \Gamma_0 \exp(-\beta\rho^2) \tag{1}$$

where Γ_0 and β are constants with $|\Gamma_0| \leqq 1$.

The reflection coefficient of the URM is assumed to be unity. (A reflection coefficient different than unity can readily be included in the solution.)

The integral equations for this resonator are obtained in a manner analogous to a URM resonator, by imposing the condition that the field should reproduce itself after a round trip. With the azimuthal dependence for the electric field $E(\rho, \phi) = \exp(-j_\ell\phi)F_\ell(\rho)$, the two simultaneous integral equations are:[5]

$$K_\ell^{(2)}F_\ell^{(2)}(\rho_2) = j^{\ell+1}\exp(-jkd)M\int_0^\infty F_\ell^{(1)}(\rho_1)\exp[-jM(g_1\rho_1^2 + g_2\rho_2^2)/2] \cdot J_\ell(M\rho_1\rho_2)\rho_1\, d\rho_1, \tag{2}$$

$$K_\ell^{(1)}F_\ell^{(1)}(\rho_1) = j^{\ell+1}\exp(-jkd)M\Gamma_0\exp(-\beta\rho_1^2)\int_0^\infty F_\ell^2(\rho_2) \cdot \exp[-jM(g_1\rho_1^2 + g_2\rho_2^2)/2]\cdot J_\ell(M\rho_1\rho_2)\rho_2\, d\rho_2, \tag{3}$$

where $F_\ell^{(1)}(\rho_1)$, $F_\ell^{(2)}(\rho_2)$ are the radial field distributions at (M1) and (M2) respectively, $K_\ell^{(1)}$ and $K_\ell^{(2)}$ are the associated eigenvalues, J_ℓ is a Bessel function of order ℓ, $M = 2\pi/\lambda d$, λ is the free-space wavelength and

$$g_1 = \left(1 - \frac{d}{R_1}\right), \tag{4}$$

$$g_2 = \left(1 - \frac{d}{R_2}\right). \tag{5}$$

The integral equations (2) and (3) are solved by using the self-reciprocal properties of the Laguerre functions on the Hankel transform.[6,7] These properties are

$$\int_0^\infty x^{v+1} \exp(-\beta x^2) L_n^v(\alpha x^2) J_v(xy)(xy)^{\frac{1}{2}}\, dx$$

$$= 2^{-v-1} y^{v+\frac{1}{2}} (\beta - \alpha)^n \beta^{-n-v-1} \exp(-y^2/4\beta) L_n^v\left(\frac{\alpha y^2}{4\beta(\alpha - \beta)}\right) \tag{6}$$

where L_n^ℓ is a Laguerre function of order ℓ, n.

Based on equation (6), the modal solutions to the integral equations are:

$$F_\ell^{(1)}(\rho_1) = \exp(-\gamma_1 \rho_1^2/2) L_n^\ell(\alpha_1 \rho_1^2)(\sqrt{\alpha_1}\ \rho_1)^\ell, \tag{7}$$

$$F_\ell^{(2)}(\rho_2) = \exp(-\gamma_2 \rho_2^2/2) L_n^\ell(\alpha_2 \rho_2^2)(\sqrt{\alpha_2}\ \rho_2)^\ell. \tag{8}$$

After some algebraic manipulations, the following relations are obtained for the parameters.

$$\gamma_1 = \alpha_1 + \beta, \tag{9}$$

$$\alpha_1^2 = \frac{M^2}{4g_2^2} + \left[\beta + jM\left(g_1 - \frac{1}{2g_2}\right)\right]^2. \tag{10}$$

It is convenient to express α_1 in terms of a complex trigonometric function as follows

$$\alpha_1 = \frac{M}{2g_2} \cosh \delta \tag{11}$$

with $\delta = \Lambda + j\Delta$. In equations (9) and (10), Λ and Δ are related to the resonator geometry and reflectivity parameters by

$$\sinh \Lambda \cos \Delta = \frac{2g_2\beta}{M}, \tag{12}$$

$$\cosh \Lambda \sin \Delta = (2g_1g_2 - 1). \tag{13}$$

Furthermore

$$\gamma_2 = \alpha_2, \tag{14}$$

$$\alpha_2 = Mg_2 \frac{(\cos \Delta + j \sinh \Lambda)}{\sin \Delta + \cosh \Lambda}. \tag{15}$$

The associated eigenvalues $K_\ell^{(1)}$ and $K_\ell^{(2)}$ are:

$$K_\ell^{(1)} = \Gamma_0 \exp(-jkd)_j n \left[\frac{1 + j \exp(-\delta)}{2g_2}\right]^{\ell+1} \exp(-n\delta), \tag{16}$$

$$K_\ell^{(2)} = \exp(-jkd)j^n \left[\frac{j2g_2}{\exp(\delta) + j}\right]^{\ell+1} \exp(-n\delta). \tag{17}$$

The eigenvalue K_ℓ which gives the decrease of the reflected field after a double pass is the product of the above two eigenvalues given by equations (16) and (17).

$$K_\ell = K_\ell^{(1)}K_\ell^{(2)} = (-1)^n j^{\ell+1} \exp(-j2kd)\Gamma_0 \exp[-(2n + \ell + 1)\delta]. \tag{18}$$

The eigenvalues K_ℓ are exponentially decreasing with ℓ, n. The largest eigenvalue is obtained for $n = \ell = 0$, corresponding to the fundamental $TEM_{0,0}$ mode. The next eigenvalue corresponds to the $TEM_{1,0}$ mode ($\ell = 1$, $n = 0$). Since the eigenvalues are related to the power loss, the fundamental mode selectivity will depend primarily on the eigenvalues for the $TE_{0,0}$ and $TE_{1,0}$ modes.

It is of interest to examine the special case $g_2 = 1$, which corresponds to a resonator with a perfectly reflecting planer mirror M2. This resonator is completely equivalent to a symmetrical resonator consisting of two identical VRM separated by $2d$. Both the eigenvalues and the fields are the same with the fields beyond d being equal to the reflected fields of the nonsymmetrical resonator.

The modes of the nonsymmetrical resonator are orthogonal at the uniform mirror M2, since $\gamma_2 = \alpha_2$. Howerer, at the VRM neither the incident modes nor the reflected modes are orthogonal. This is shown in Appendix A. In addition it is shown that for any particular mode, the ratio of the reflected to the incident power at the VRM is precisely equal to the absolute value square of the eigen value K_ℓ. Physically this condition corresponds to conservation of power.

2.2 *Stability Criteria*

For a resonator made to be stable, it is necessary that the exponential factors γ_1 and γ_2 in equations (7) and (8) be finite and have a positive

real part. Both these factors are dependent on cos Δ and g_2 . The limits of the stability regions are thus: (a) $g_2 = 0$ and (b) cos $\Delta = 0$. The second condition can be expressed in terms of the resonator parameters by using equation (13).

$$\cos \Delta = \left[1 - \left(\frac{2g_1g_2 - 1}{\cosh \Lambda}\right)^2\right]^{\frac{1}{2}} \tag{19}$$

and the second limit of the stability region is

$$g_2 = \frac{1 \pm \cosh \Lambda}{2g_1}. \tag{20}$$

Equation (20) contains the special case of the uniform reflectivity resonator (cosh $\Lambda = 1$). For this special case equation (20) reduces to the stability criterion derived by G. D. Boyd and H. Kogelnik.[8]

In Fig. 2 illustrative stability diagrams are shown as a function of g_1 and g_2 with exp (2Λ) as a parameter. (The choice of this parameter is discussed subsequently.)

A few special cases are considered

(*i*) $g_1 = 0$.
This resonator is stable for all values of g_2 , except $g_2 = 0$.

(*ii*) $g_2 = 0$.
This resonator is unstable independent of the curvature of M1.

(*iii*) $g_1 = g_2 = 0$.
This is the very special case of the confocal resonator and is in general unstable, except for a URM resonator ($\beta = 0$).

(*iv*) $g_1 = g_2 = 1$.
This is the Fabry-Perot resonator and is stable with a variable reflectivity mirror.

2.3 *The Threshold-Gain Ratio*

To sustain oscillations in a laser resonator a necessary condition is that the active medium should have enough gain such that after a double transit the field has the same amplitude. This condition can be written in terms of the eigenvalues of the resonator modes as[9]

$$G\,|K_\ell|^2 = 1 \tag{21}$$

where G is the power gain per double transit.

In particular for the $TEM_{0,0}$ and $TM_{1,0}$ modes, equation (21) can be written using equation (18) as:

$$G_{0,0}\Gamma_0^2 \exp(-2\Lambda) = 1, \tag{22}$$

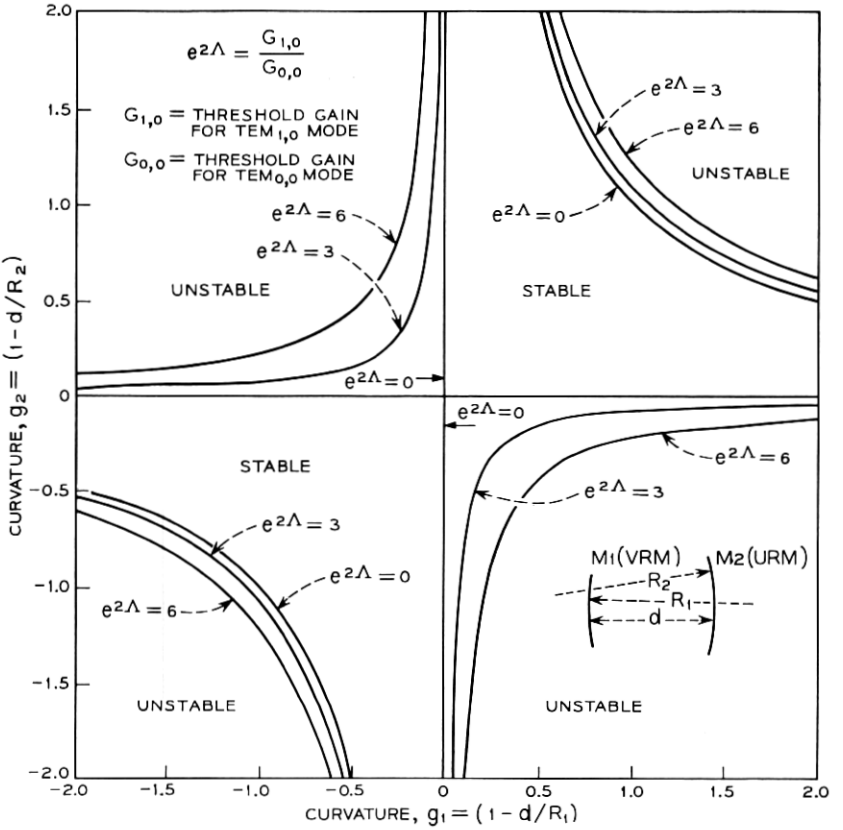

Fig. 2—Stability diagrams.

$$G_{1,0}\Gamma_0^2 \exp(-4\Lambda) = 1, \tag{23}$$

where $G_{0,0}$ and $G_{1,0}$ is the threshold-power gain required for oscillation in the respective modes. A quantity of interest is the threshold-gain ratio, t defined by:

$$t = \frac{G_{1,0}}{G_{0,0}} = \exp(2\Lambda). \tag{24}$$

This ratio is a measure of the gain tolerance required for oscillation in the dominant $TEM_{0,0}$ mode, and is independent of Γ_0.

The threshold-gain ratio may also be expressed in terms of the loss per round trip $L_{0,0}$ for the $TEM_{0,0}$ mode. Since

$$L_{0,0} = 1 - \Gamma_0^2 \exp(-2\Lambda). \tag{25}$$

The threshold-gain ratio can be written,

$$t = \frac{\Gamma_0^2}{1 - L_{0,0}}. \tag{26}$$

Equation (26) is shown in Fig. 3 as a function of $L_{0,0}$. It is evident that the threshold-gain ratio increases with the loss and hence better mode discrimination is obtained as the loss increases.[1] Furthermore, the power output is related to the power loss per transit. Therefore different values of Γ_0^2 can be used to shape the spatial distribution of the power output.

A comparison is made (similar to that in Ref. 1) between the threshold-gain ratio of a Fabry-Perot resonator with URM and a resonator with VRM as a function of the loss per transit.

Based on the Vainshtein resonator theory[10] for the URM resonator the threshold gain ratio

$$t = \left(\frac{1}{1 - L_d}\right)^{[(\nu_{1,0}/\nu_{0,0})^2 - 1]} \tag{27}$$

where L_d is the diffraction loss for the $TE_{0,0}$ mode and $\nu_{n,0}$ is the first nonzero root of $J_n(\nu) = 0$.

Equation (27) is also plotted in Fig. 3. It is evident from this figure that the threshold-gain ratio as a function of the diffraction loss is higher for the Fabry-Perot resonator with uniform mirrors than the corresponding ratio for the variable reflectivity resonator. This con-

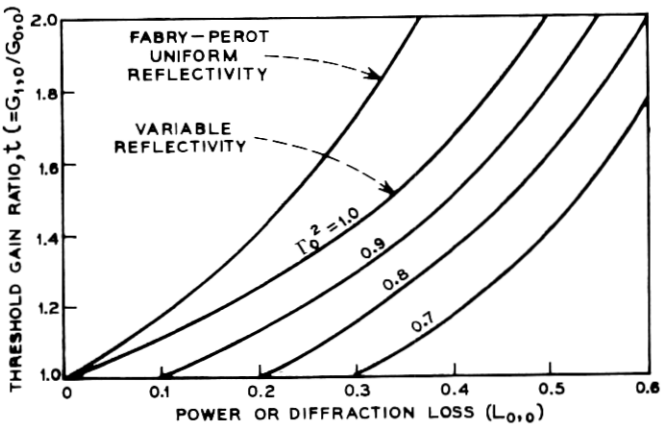

Fig. 3—Comparison of uniform and variable reflectivity mirror resonators.

clusion was previously reached by Vlasov and Talanov,[1] who also showed that the highest threshold-gain ratio is obtained with confocal resonators with uniform reflectivity mirrors. However, the high threshold-gain ratio is only of primary importance for low-gain lasers, where the output power obtained by partial transmittivity of the mirrors is only a fraction of the power lost by diffraction. For high-gain lasers, however, the mode utilization volume is of prime importance and the threshold-gain ratio can be kept at a specified level by the proper choice of the loss per pass. For such lasers the resonators with variable reflectivity mirrors have the advantage that the power loss which is necessary for mode discrimination can also be utilized as the power output. The mode volume utilization aspect is discussed later.

III. COMPUTED $TEM_{0,0}$ MODE CHARACTERISTICS

3.1 *Spot Sizes*

The $TEM_{0,0}$ mode is of particular interest since it is the fundamental mode having the highest eigenvalue and hence the lowest loss. For this mode the field distributions are gaussian with quadratic phase variations. Specifically the field distributions for the $TE_{0,0}$ mode from equations (7) and (8) are

$$F_{i1} = \exp\left\{-\frac{M}{4g_2}\left[\exp(-\Lambda)\cos\Delta + j\sinh\Lambda\sin\Delta\right]\rho_1^2\right\}, \tag{28}$$

$$F_{r1} = \exp\left\{-\frac{M}{4g_2}\left[\exp(\Lambda)\cos\Delta + j\sinh\Lambda\sin\Delta\right]\rho_1^2\right\}, \tag{29}$$

$$F_{r2} = \exp\left\{-\frac{Mg_2}{2}\left(\frac{\cos\Delta + j\sinh\Lambda}{\sin\Delta + \cosh\Lambda}\right)\rho_2^2\right\}, \tag{30}$$

where F_{i1} and F_{r1} are the field distributions of the incident and reflected fields at M1, and F_{r2} is the reflected field at M2.

The reflection coefficient can be expressed in terms of Λ and Δ is by using equation (12) as

$$\Gamma = \Gamma_0 \exp\left(-M/2g_2 \sinh\Lambda\cos\Delta\,\rho_1^2\right). \tag{31}$$

The eigenvalue for the $TEM_{0,0}$ mode is

$$K_0 = \Gamma_0 \exp(-j2kd)\exp\left[-(\Lambda + j\psi_0)\right] \tag{32}$$

with

$$\psi_0 = \frac{\pi}{2} - \cos\Delta. \tag{33}$$

The amplitudes of the field distributions at the mirrors are completely characterized by the spot sizes defined by that radius when the above quantities assume the value of $1/e$. Since the exponents in equations (28) through (31) are proportional to M, it is convenient to introduce the Fresnel numbers of the spot sizes. For example, for F_{i1} the spot size is defined by

$$\frac{M}{4g_2} \exp(-\Lambda) \cos \Delta \rho_{i1}^2 = 1 \tag{34}$$

or

$$N_{i1} = \frac{2}{\pi} \frac{\exp(\Lambda)}{\cos \Delta} g_2 \tag{35}$$

where $N_{i1} = \rho_{i1}^2/\lambda d$ is the Fresnel number. The corresponding Fresnel numbers of equations (29) through (31), N_{r1} , N_{r2} , N_m are defined in an analogous manner.

The above Fresnel numbers have been computed as a function of the threshold-gain ratio $t = \exp(2\Lambda)$, with the radii of curvature as parameters. Two types of resonators were considered: (*i*) a resonator with a uniformly reflecting plane mirror and a curved mirror with variable reflectivity with radius of curvature as a parameter, and (*ii*) a resonator with plane mirror with a variable reflectivity and a uniformly reflecting mirror with radius of curvature as a parameter.

For resonator (*i*), Figs. 4 through 6 show the Fresnel numbers of:

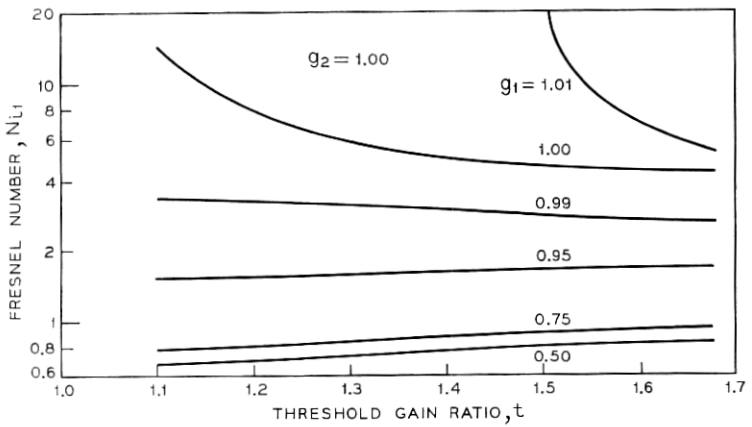

Fig. 4—Spot size of incident beam, N_{i1}.

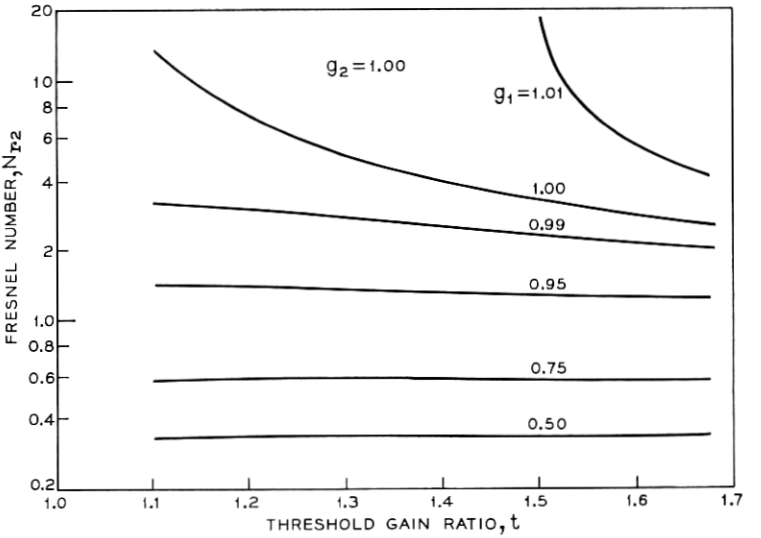

Fig. 5—Spot size of reflected beam, N_{r2}.

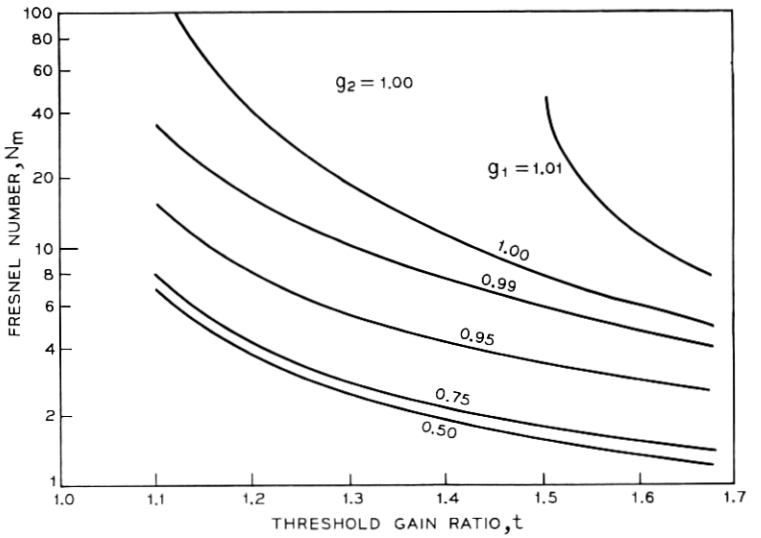

Fig. 6—Spot size of variable reflectivity mirror, N_m.

the incident beam at M1, N_{i1}, the reflected beam at M2, N_{r2} and the Fresnel number of the variable reflectivity mirror N_m. Figure 7 shows the phase of the eigenvalue ψ_0, equation (33). Figures 8 through 10 show the corresponding quantities for the type (*ii*) resonator. The phase ψ_0 is the same as in Fig. 7 but with g_1 and g_2 interchanged.

A comparison of the characteristics for the two types of resonators shows that the most pronounced differences are when either of the mirrors have curvatures g_1 or $g_2 = 0.5$. Larger spot sizes are obtainable with the type (*i*) resonator. The Fabry-Perot resonator for which g_1 and $g_2 = 1.0$ is a special case for both types. It also may be noted that a large increase in the spot size occurs when one of the mirrors is slightly convex, e.g., g_1 or $g_2 = 1.01$. This increase is caused by the curvature of the resonator mirror which approaches the unstable region, Fig. 2.

For a finite resonator, the resonator diameter will be limited by the minimum obtainable reflectivity at the mirror edges. At the spot-size diameter the reflection coefficient of the mirror has the value $1/e$. The spot-size diameter may be considered as a measure for the diameter of the VRM. The Fresnel number of the spot size of the incident beam, which for a variety of geometries is the maximum spot size of the beam along the resonator is related to the Fresnel number of the

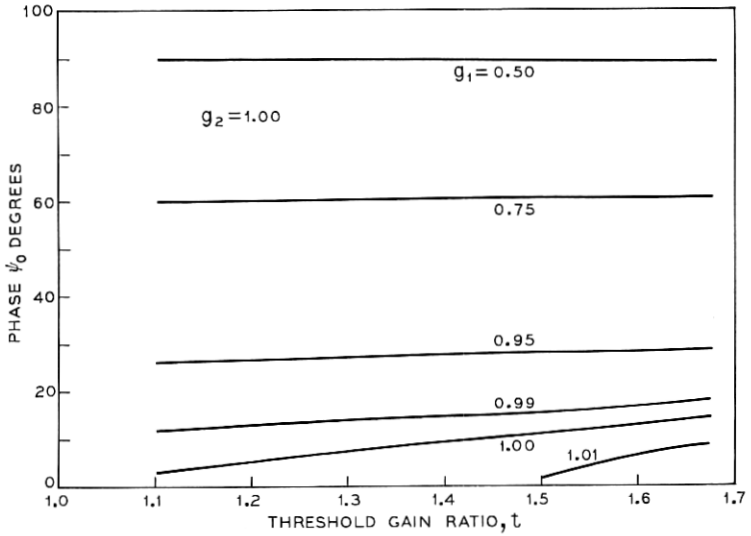

Fig. 7—Phase of the eigenvalue, $K_{0,0}$.

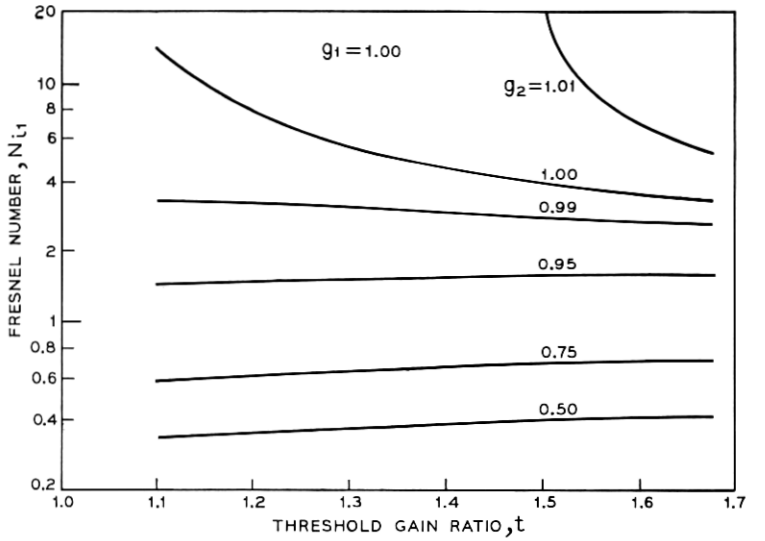

Fig. 8—Spot size of incident beam, N_{i1}.

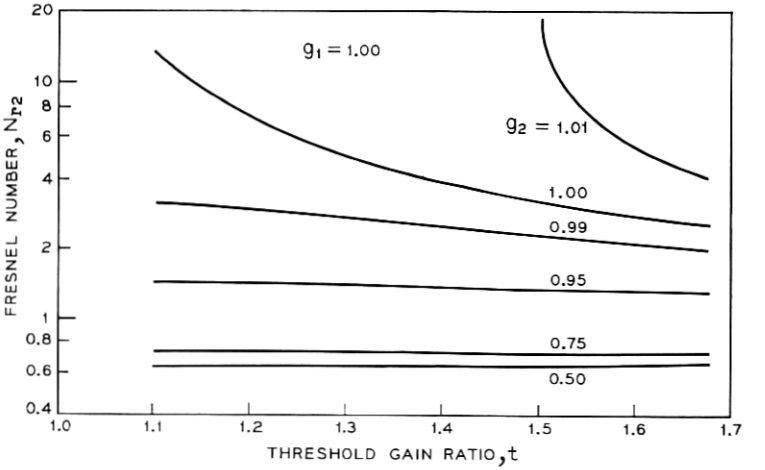

Fig. 9—Spot size of reflected beam, N_{r2}.

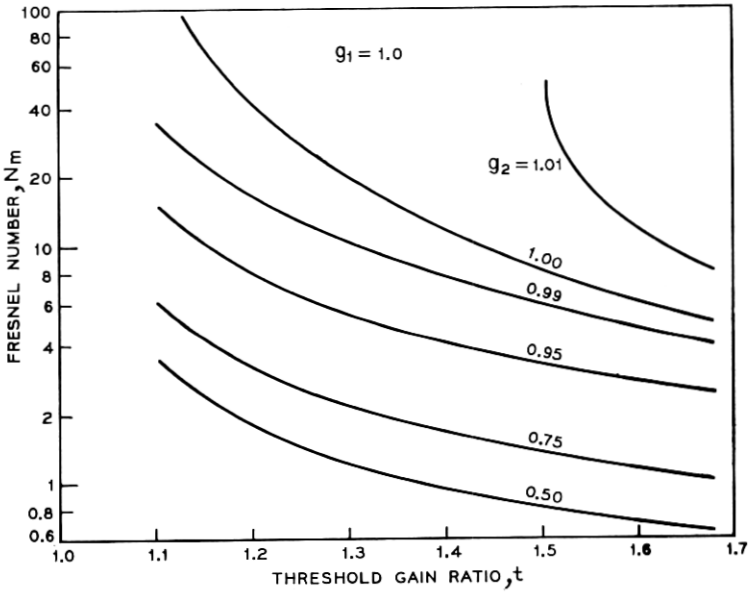

Fig. 10—Spot size of variable reflectivity mirror, N_m.

mirror spot size by:

$$\frac{N_{i1}}{N_m} = [\exp(2\Lambda) - 1] = t - 1. \tag{36}$$

For a resonator with finite dimensions to be a good approximation to the infinite resonators, it is necessary that beam power outside the mirrors be small. To obtain an estimate of this power, a resonator is assumed with a diameter equal to the mirror spot size diameter.

The ratio p, of the incident power outside the mirror spot-size diameter to the total incident power is from equations (28) and (1) given by

$$p = \frac{\int_{1/\sqrt{\beta}}^{\infty} \exp[-M/2g_2 \exp(-\Lambda) \cos \Delta\rho_1^2]\rho_1 \, d\rho_1}{\int_0^{\infty} \exp[-M/2g_2 \exp(-\Lambda) \cos \Delta\rho_1^2]\rho_1 \, d\rho_1}. \tag{37}$$

After performing the integration and substituting equation (12), this ratio can be written as

$$p = \exp\{-2/[\exp(2\Lambda) - 1]\}. \tag{38}$$

It readily follows from equation (38) that for a threshold-gain ratio $t = \exp(2\Lambda)$ smaller than 1.43, p is less than one percent.

A comparison is made between the characteristics of Fabry-Perot resonators with one large (such that the diffraction loss is negligible) uniformly reflecting mirror and with the other mirror being either of uniform or variable reflectivity. For the resonator with VRM, the Fresnel number for a given diffraction loss has twice the value than that if both mirrors are of the same size. Figure 11 shows the Fresnel number of the uniform mirror as a function of threshold-gain ratio. The curve is based on the Vainshtein resonator theory.[10] In the same figure is also shown the Fresnel number of the spot size of the incident field N_{i1}. It is evident from this figure that the spot-size diameter at the VRM is considerably larger than the diameter of the uniform reflectivity mirror for the same values of t. As an example the special case of a resonator with a uniform mirror with a Fresnel number of two is considered. For this resonator, the field at the mirror has been computed by T. Li.[5] Though the field distribution for the $TEM_{0,0}$ is not gaussian, for comparison purposes the Fresnel number of the spot size (based on the $1/e$ value for the field) is estimated to be about 1.6. For the same value of t the Fresnel number of spot size for the

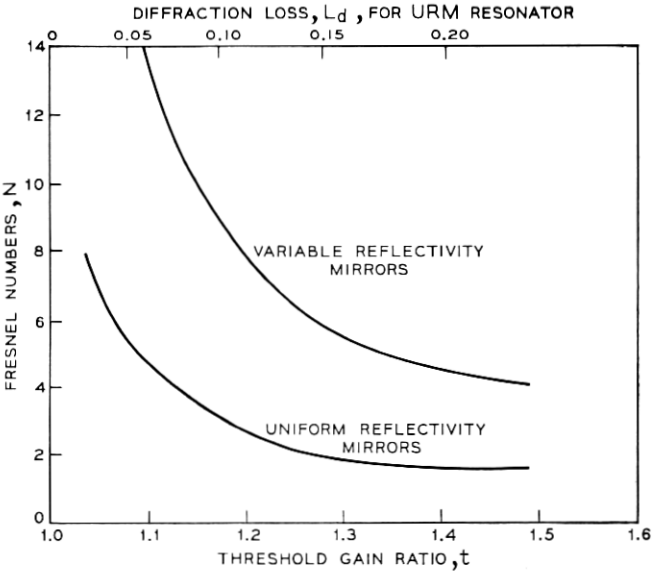

Fig. 11—Comparison of the beam sizes of Fabry-Perot resonators.

VRM resonator is 5.2. For lower values of t the difference in the spot sizes is even more pronounced. One of the advantages of VRM resonator is therefore the larger spot sizes and hence the large potential for mode volume utilization.

3.2 *Field Distributions in the Resonator*

For efficient mode volume utilization, the field along the resonator should be reasonably uniform. The uniformity of the fields is strongly dependent on the mirror curvatures. Referring to Fig. 1, let $B1$ be the reflected beam from M1 and $B2$ the reflected beam from M2. The functional dependence of the two beams on the longitudinal z coordinate has been obtained from the fields at the mirrors, and is given by the following equations

$$B1 = \exp\left[-\gamma_1(z)\right] \frac{\rho_1^2}{2}, \tag{39}$$

$$B2 = \exp\left[-\gamma_2(z)\right] \frac{\rho_2^2}{2}, \tag{40}$$

with

$$\gamma_1(z) = \frac{M\left\{2g_2\left(\frac{d}{z}\right)^2 \exp(\Lambda)\cos\Delta + j\frac{d}{z}\left[(\exp(\Lambda) + a\sin\Delta)^2 + a^2\cos^2\Delta - 2g_2\frac{d}{z}(\exp(\Lambda)\sin\Delta + a)\right]\right\}}{(\exp(\Lambda) + a\sin\Delta)^2 + a^2\cos^2\Delta}, \tag{41}$$

$$a = 1 + 2g_2\left(\frac{d}{z} - 1\right), \tag{42}$$

and

$$\gamma_2(z) = \frac{M\left[2g_2\left(\frac{d}{d-z}\right)^2 \exp(\Lambda)\cos\Delta + j\left(\frac{d}{d-z}\right)\left\{(\exp(\Lambda)b - \sin\Delta)^2 + \cos^2\Delta + \frac{d}{d-z}\left[\exp(2\Lambda)b + 2\exp(\Lambda)\sin\Delta(g_2 - 1) - 1\right]\right\}\right]}{\left[\exp(\Lambda)\left(b + \frac{d}{d-z}\right) + \left(\frac{d}{d-z} - 1\right)\sin\Delta\right]^2 + \left(\frac{d}{d-z} - 1\right)^2\cos^2\Delta} \tag{43}$$

with

$$b = (2g_2 - 1). \tag{44}$$

The real part of equations (41) and (43) has been evaluated as a function of z, in terms of the spot-size Fresnel number $N_1(z)$ and $N_2(z)$ defined in accordance with equation (34) as $N_{1,2}(z) = 2/\gamma_{1,2}(z)\lambda d$. For a resonator with $g_2 = 1.0$, Fig. 12 shows the spot-size Fresnel number as a function z/d for a number of parameters.

It is characteristic of resonators with VRM, that minimum-beam spot size even for symmetrical resonators does not occur at half the mirror spacings in contrast to resonators with uniform reflectivity mirrors. In Fig. 12 this characteristic is particularly evident for the equivalent confocal resonator $g_1 = 0.5$.

The uniformity of the beams along the resonator increases with the

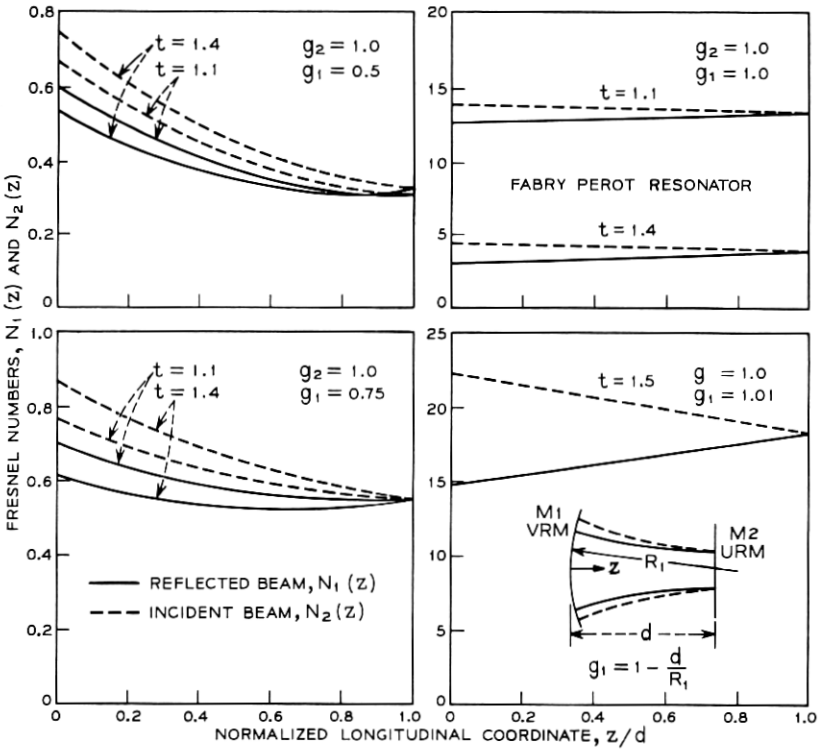

Fig. 12—Spot size of the beams along the resonator.

increasing value of g_1 up to $g_1 = 1.0$ which corresponds to the Fabry-Perot resonators. For this resonator the beams are most uniform. For the higher value of $g_1 (g_1 = 1.01)$ the uniformity of the beams within the resonator decreases.

3.3 *Minimum Spot Sizes*

The uniformity of the beams within the resonator depends on the locations of the minimum spot-size diameters. The beam diameters are more uniform if the virtual minimum spot-size diameters occur at distances, away from the mirrors, which are large in comparison to the separation of the mirrors. The positions of the minimum spot sizes are obtained either by determining the maxima or by setting the imaginary parts of equations (41) and (43) equal to zero. Either condition gives the same result (i.e., at the minimum spot-size positions the beams have constant phase).

The minimum positions for the two beams $(z_1/d)_{\min}$ and $(z_2/d)_{\min}$ are:

$$\left(\frac{z_1}{d}\right)_{\min} = 2g_2 \frac{[2g_2 - 1 - \exp(\Lambda)\sin\Delta]}{[\exp(2\Lambda) + 2(1 - 2g_2)\exp(\Lambda)\sin\Delta + (1 - 2g_2)^2]} \tag{45}$$

and

$$\left(\frac{z_2}{d}\right)_{\min} = 2g_2 \exp(\Lambda) \frac{[\exp(\Lambda)(2g_2 - 1) - \sin\Delta]}{[\exp(2\Lambda)(1 - 2g_2)^2 + 2(1 - 2g_2)\exp(\Lambda)\sin\Delta + 1]}. \tag{46}$$

The Fresnel numbers of the minimum spot sizes $[N_1(z)]_{\min}$ and $[N_2(z)]_{\min}$ are:

$$[N_1(z)]_{\min} = \frac{2g_2 \cos\Delta \exp(\Lambda)}{\pi[\exp(2\Lambda) + 2(1 - 2g_2)\exp(\Lambda)\sin\Delta + (1 - 2g_2)^2]} \tag{47}$$

and

$$[N_2(z)]_{\min} = \frac{2g_2 \cos\Delta \exp(\Lambda)}{\pi[\exp(2\Lambda)(1 - 2g_2)^2 + 2(1 - 2g_2)\exp(\Lambda)\sin\Delta + 1]}. \tag{48}$$

The minimum positions and minimum spot sizes have been computed for a resonator with a VRM and variable radius of curvature and a uniform plane mirror $g_2 = 1.0$. Since this resonator is equivalent to a symmetrical resonator with two VRM, the two minimum positions are mirror images with respect to the uniform mirror, and the minimum spot sizes are the same. For this resonator

$$[N_1(z)]_{\min} = [N_2(z)]_{\min} = \frac{1}{\pi} \frac{\cos\Delta}{[\cosh\Lambda - \sin\Delta]}. \tag{49}$$

For specified Λ equation (49) has a maximum for $\cosh \Lambda \sin \Delta = 1$, which from equation (13) corresponds to the Fabry-Perot resonator ($g_1 = g_2 = 1.0$). The corresponding Fresnel number N_M is:

$$N_M = \frac{1}{\pi \sinh \Lambda}. \tag{50}$$

Figure 13 shows $(z_2/d)_{\min}$ as a function of g_1 with $t = \exp(2\Lambda)$ as a parameter. As g_1 increases, so does $(z_2/d)_{\min}$ assuming relatively large values in the vicinity of $g_1 = 1.0$. The large values of $(z_2/d)_{\min}$ explain the uniformity of the beams in the Fabry-Perot resonator. Figure 14 shows the dependence of the minimum spot on the mirror curvature g_1 with t as a parameter.

3.4 *Dependence of the Spot Sizes on the Curvatures of Spherical Mirrors*

The previous calculations show that large spot sizes are obtainable in the vicinity of the instability region. How critically the spot sizes depend on mirror curvatures is of importance.

The Fresnel number of the spot size for the incident beam N_{fi} is directly related to the Fresnel number of the VRM by equation (36).

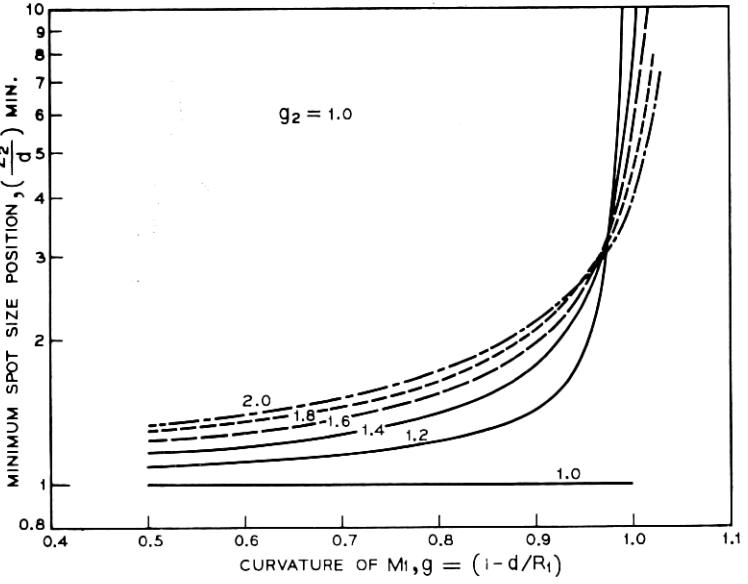

Fig. 13—Location of the minimum spot size.

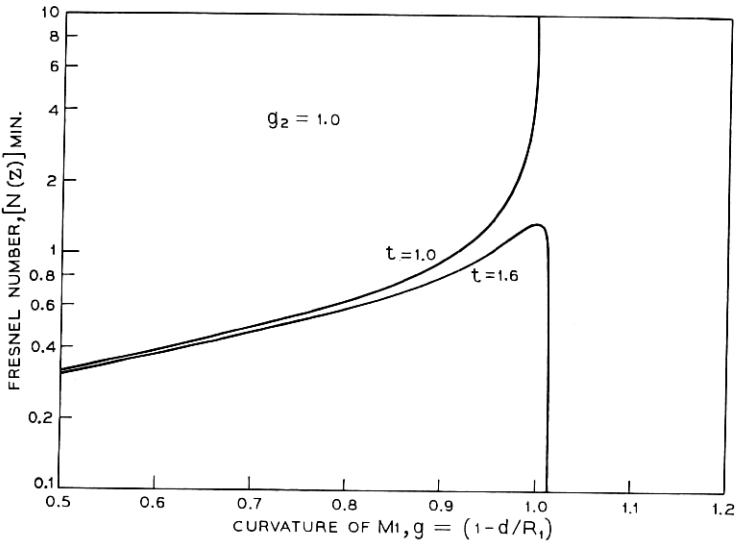

Fig. 14—Fresnel number of minimum spot size as a function of curvature of M1.

Equations (12) and (13) give the relation between the Fresnel number of VRM, the mirror curvature and Λ. Solving these equations for g_1 gives:

$$g_1 = \frac{\text{ctnh } \Lambda[(\pi N_m \sinh \Lambda)^2 - g_2^2]^{\frac{1}{2}} + \pi N_m}{2\pi g_2 N_m} \tag{51}$$

where N_m is related to β in equation (1) by $N_m = (1/\beta\lambda d)$.

Equation (51) has been computed as a function of g_2 with t as a parameter. Figures 15 through 18 show the computed characteristics for $N_m = 10,20,40,100$.

The critical dependence of the beam spot size N_{i1} on the mirror curvatures is evident from these figures, particularly as N_m increases. A small change in g_1 or g_2 results in a large change in t and there is a very large change in the beam spot size N_{i1} for a specified N_m.

The conclusion based on these computations is that though large Fresnel numbers for the beam spot sizes are in principle possible, the critical tolerance requirements for the mirror curvatures may set a practical limit on spot sizes relative to those obtainable with a Fabry-Perot resonator with one VRM.

3.5 *Resonator Design*

As an application, a resonator design is considered for a CO_2 laser. In view of the realizable high gain per pass, the power loss per pass and the related power output should be large. A Fabry-Perot resonator with a VRM mirror seems to be most suitable for this application. The remaining parameter to be specified is the threshold-gain ratio, t. This ratio should be as low as possible in order to obtain large beam diameters (see Fig. 11). For the fundamental $TEM_{0,0}$ mode operation, the limitation on t is based on the accuracy with which the gain can be controlled. A value of t of 1,2 is assumed.

Using the above parameters in equations (28) and (31) (Figs. 4 and 6) the Fresnel number of the spot size of the VRM is 38.35 and that of the incident beam at the VRM is 7.65. For a resonator with length $d = 100$ cm and for a wavelength $\lambda = 10^{-3}$ cm (10 micron), the radius of the spot size of the VRM, $a_m = 1.95$ cm.

Some of the characteristics of this resonator are shown in Fig. 19. Illustrated is the dependence of the power-reflection coefficient Γ^2 as a function of the normalized radius ρ/a_m. Also shown is the normalized-incident power density at the VRM, and power loss density at the VRM for different values of the reflectivity at the center, Γ_0^2, as functions of

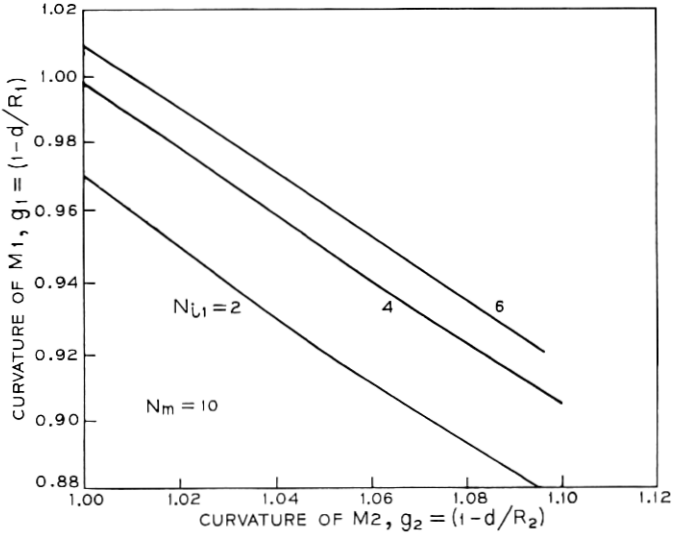

Fig. 15—Relation between mirror curvature parameters g_1 and g_2 and Fresnel number N_{i1} of spot size at M1.

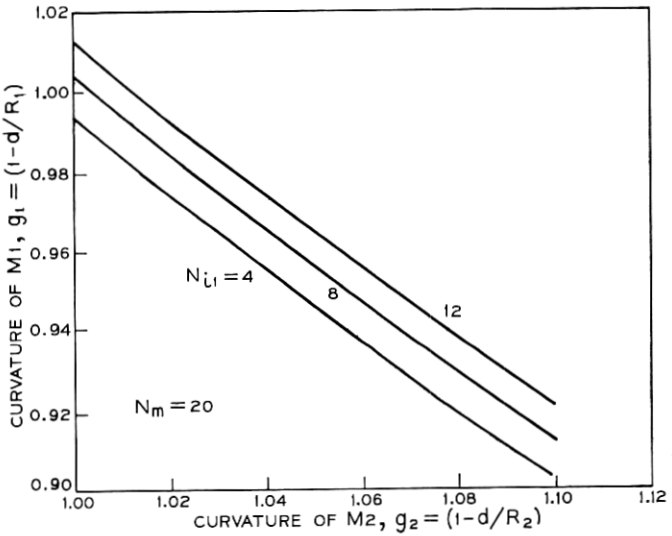

Fig. 16—Relation between mirror curvature parameters g_1 and g_2 and Fresnel number N_{i1} of spot size at M1.

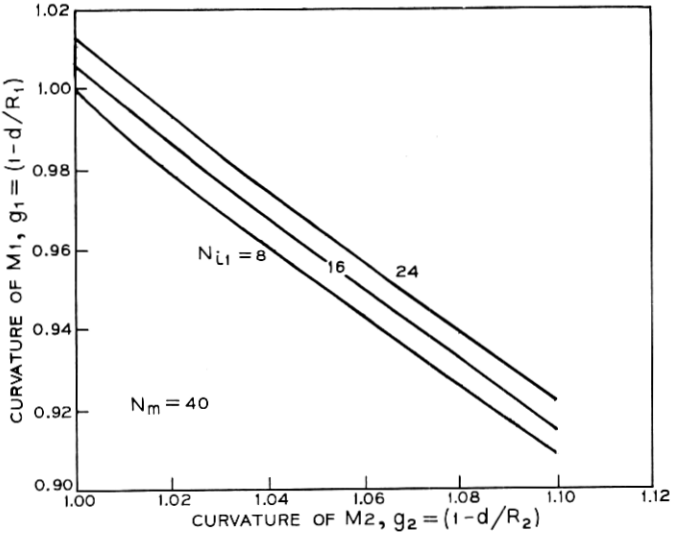

Fig. 17—Relation between mirror curvature parameters g_1 and g_2 and Fresnel number N_{i1} of spot size at M1.

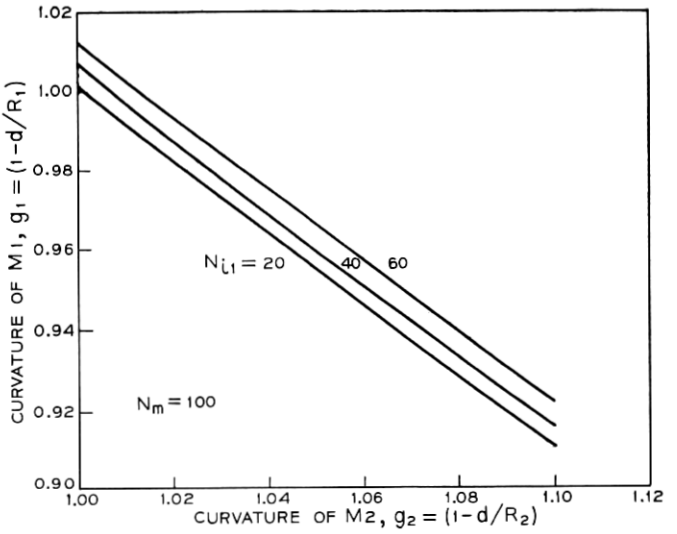

Fig. 18—Relation between mirror curvature parameters g_1 and g_2 and Fresnel number N_{i1} of spot size at M1.

ρ/a_m. The power-loss density is the laser-power output when the absorptivity of the VRM is zero. Figure 20 shows the ratio of the power loss to the incident power as a function ρ/a_m with Γ_0^2 as parameters.

The actual diameter of the VRM can presently be determined only by assuming that a finite resonator will behave similarly to a resonator with infinite mirrors when the beam power outside a certain diameter is small. For the resonator considered, 0.5 percent of the incident beam power is contained outside the mirror radius of 0.73 a_m and one percent outside the radius 0.68 a_m which corresponds for the above value of a_m to 1.41 cm and 1.31 cm radii. For a resonator with a VRM of radius a_m the perturbation of the fields should therefore be very small.

IV. CONCLUSIONS

The characteristics of optical resonators with gaussian radial variations of the mirror reflectivities have been investigated. These variable reflectivity mirror (VRM) resonators seem to be particularly suitable for high-gain and high-power laser application such as the 10.6 micron CO_2 laser. For the fundamental $TEM_{0,0}$ mode generation, these resonators have the advantage in comparison to conventional resonators that larger beam spot sizes are obtainable (with better mode-volume

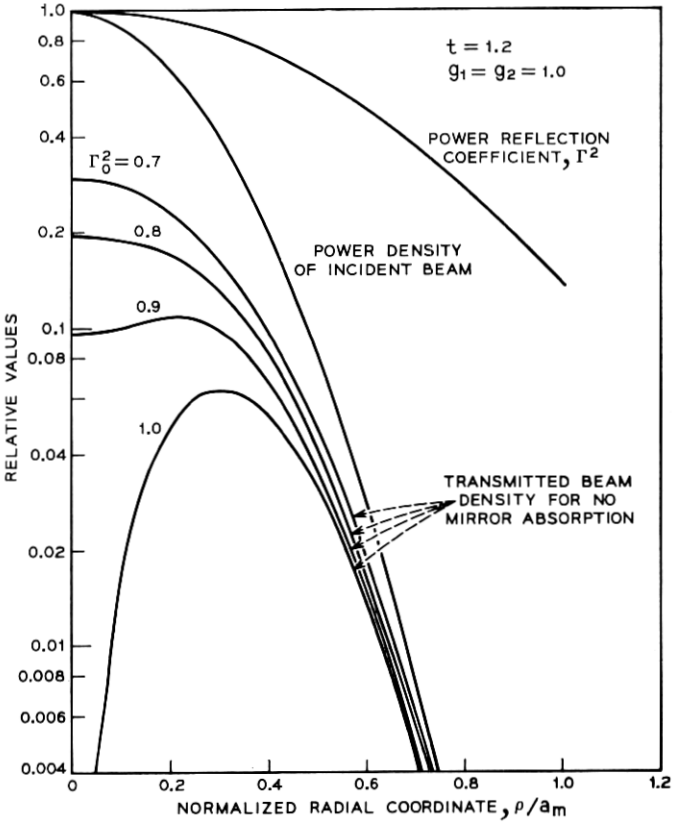

Fig. 19—Power distribution at the variable reflectivity mirror.

utilization) and the power loss necessary for mode discrimination can be utilized as the power output.

The factors limiting the spot are the threshold-gain ratio and the mirror-curvature tolerances.

The Fabry-Perot resonator with a VRM is stable and furthermore the field distribution along the resonator is more uniform in diameter relative to other resonator geometries. A specific design of such a resonator with a gain threshold ratio ($G_{1,0}/G_{0,0}$) of 1.2 shows that a spot size Fresnel number of 7.65 with a power loss (or power output depending on the absorptivity of the mirrors) as high as 40 percent of the incident power are obtainable.

In this investigation it was assumed that the mirrors are infinite.

The results presented should be a good approximation to a finite resonator when the beam power outside a certain circular region has a negligible value (say less than one percent).

V. ACKNOWLEDGMENTS

The author gratefully acknowledges the valuable comments and suggestions of N. Amitay and H. G. Cooper.

APPENDIX A

Integrals of Laguerre Functions

In order to determine the orthogonality and power relations for the modes in resonators with variable reflectivity mirrors, the following integral $I^{\ell}_{m,n}$ of product of Laguerre functions is evaluated.

$$I^{\ell}_{m,n} = 2\int_0^{\infty} \exp(-s\rho^2) L^{\ell}_m(\alpha\rho^2) L^{\ell}_n(\beta\rho^2) \rho^{2\ell+1}\, d\rho,$$

$$= \int_0^{\infty} \exp(-st) L^{\ell}_m(\alpha t) L^{\ell}_n(\beta t) t^{\ell}\, dt. \tag{52}$$

For the special case $m = n$ the integral is known.[11,12] The integral

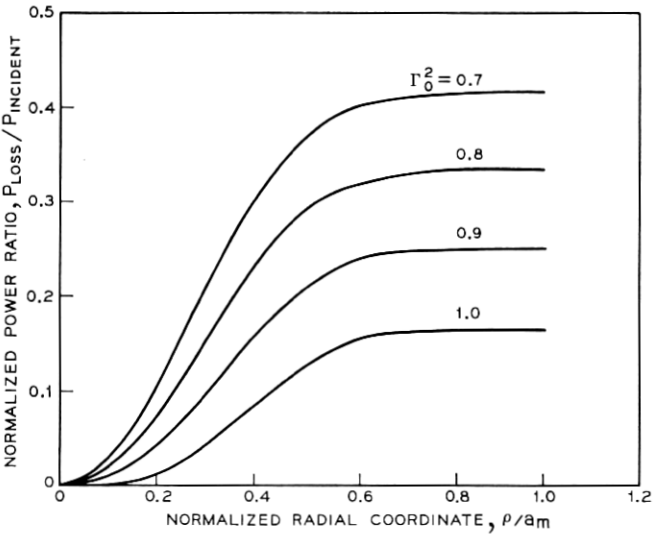

Fig. 20—Ratio of the loss to the incident beam power as a function of ρ/a_m.

(52) is evaluated by considering this integral as a Laplace transform of two functions $f_1(t)$ and $f_2(t)$ and using the Faltung relation

$$\int_0^\infty \exp(-st) f_1(t) f_2(t)\, dt = \frac{1}{2\pi j} \int_{\gamma - j\infty}^{\gamma + j\infty} F_1(z) F_2(s - z)\, dz \tag{53}$$

where $F_1(z)$ and $F_2(z)$ are the Laplace transforms of $f_1(t)$ and $f_2(t)$, γ is a constant with $\mathrm{Re}(s) > \mathrm{Re}(\gamma) > 0$.

Let

$$f_1(t) = L_m^{\ell}(\alpha t) = \sum_{k=0}^{m} (-1)^k \binom{m+\ell}{m-k} \frac{(\alpha t)^k}{k!} \tag{54}$$

and

$$f_2(t) = L_m^{\ell}(\beta t) t^{\ell}. \tag{55}$$

The Laplace transform of equations (54) and (55) are readily obtained. Furthermore with the transformation $\zeta = 1/z$ together with equation (53), equation (52) reduces to:

$$I_{m,n}^{\ell} = \frac{(n+\ell)!}{n!\, s^{m+1}} \left(-\frac{1}{\alpha}\right)^{\ell} \frac{1}{2\pi j} \oint \frac{(1-\beta\zeta)^n}{\left(\zeta - \frac{1}{s}\right)^{m+1}} [(s-\alpha)\zeta - 1]^{m+\ell}\, d\zeta. \tag{56}$$

In equation (56) the contour of integration encloses the point $\zeta = 1/s$. Equation (56) is therefore evaluated by determining the residue at $z = 1/s$, which yields

$$I_{m,n}^{\ell} = \frac{(n+\ell)!}{n!\, s^{m+1}} \left(-\frac{1}{\alpha}\right)^{\ell} \frac{d^m}{d\zeta^m} \{(1-\beta\zeta)^n [(s-\alpha)\zeta - 1]^{m+\ell}\}_{\zeta = 1/s}. \tag{57}$$

Equation (56) can be expressed in terms of Jacobi polynomials[12] by rotating and translating the coordinate system with the result that

$$I_{m,n}^{\ell} = \frac{(n+\ell)!}{n!\, s^{n+\ell+1}} (s - \alpha - \beta)^m (s-\beta)^{n-m} P_m^{\ell, n-m}(\eta) \tag{58}$$

with

$$\eta = \frac{s^2 + 2\alpha\beta - s(\alpha+\beta)}{s(s-\alpha-\beta)} \tag{59}$$

and $P_m^{\ell, n-m}$ is a Jacobi ploynomial defined by [12]

$$P_m^{a,b}(x) - \frac{(-1)^m}{2^m m!} (1-x)^{-a} (1+x)^{-b} \frac{d^m}{dx^m} [(1-x)^{a+m} (1+x)^{b+m}]. \tag{60}$$

As an application let $F_m^{\ell}(\rho)$ and $F_n^{\ell *}(\rho)$ designate the reflected fields at the VRM given by equation (7) and the* indicate the complex conjugate. The integrals which enter in the evaluation of the total reflected power due to several modes of the same index ℓ, can be written as

$$\int_0^{\infty} F_m^{\ell}(\rho) F_n^{\ell *}(\rho) \rho \, d\rho = \frac{(\alpha_1 \alpha_1^*)^{\ell/2}}{2} (I_{m,n}^{\ell})_r \tag{61}$$

where α_1 is given by equation (11). Using equations (7), (9), (11), (12) and (58), it follows that

$$\frac{(\alpha_1 \alpha_1^*)^{\ell/2}}{2} (I_{m,n}^{\ell})_r = \frac{(-1)^n (n + \ell)! \, g_2}{n! \, M \cos \Delta} \exp [-\Lambda(n + n + 1 + \ell)]$$
$$\cdot \left[1 + \frac{\sin h^2 \Lambda}{\cos^2 \Delta}\right]^{\ell/2} \left[\frac{\sin h\Lambda}{\cos \Delta} \exp (-j\Delta)\right]^{m-n} P_m^{\ell, n-m}(\eta) \tag{62}$$

with

$$\eta = -\left[1 + 2 \frac{\sin h^2 \Lambda}{\cos^2 \Delta}\right]. \tag{63}$$

For stable resonators with VRM equation (62) is not equal to zero for $m \neq n$. Hence, the total reflected power is in general not equal to the sum of the powers of the individual modes.

The reflected field $F_m^{(\ell)}(\rho)$ for any particular mode is related to the incident field $F_m^{(\ell)}(\rho)_i$ by reflection coefficient (1). The evaluation of the corresponding integral (61) for the incident fields yields the same value for η. Furthermore setting $m = n$ the following relation if obtained

$$\frac{(I_{n,n}^{\ell})_r}{(I_{n,n}^{\ell})_i} = \Gamma_0^2 \exp [-2\Lambda_0(2n + \ell + 1)] = |K_{\ell}|^2. \tag{64}$$

The meaning of equation (64) is that the ratio of the reflected to incident power for a particular mode is precisely equal to absolute value of the eigenvalue squared.

REFERENCES

1. Vlasov, S. N., and Talanov, V. I., "Selection of Axial Modes in Open Resonators," Radio Eng. and Elec. Phys., *10,* No. 3 (March 1965), pp. 469–470.
2. Vakhimov, N. G., "Open Resonators With Mirrors Having Variable Reflection Coefficients," Radio Eng. and Elec. Phys., *10,* No. 9 (September 1965), pp. 1439–1446.
3. Kumagai, N., et. al., "Resonant Modes in a Fabry-Perot Resonator Consisting of Nonuniform Reflectors," Elec. and Comm. Japan, *49,* No. 7 (July 1966), pp. 1–8.

4. Suematsu, Y., et al., "A Light Beam Waveguide Using Gaussian Mode Filters," Elec. and Comm. in Japan, *51-B,* No. 4 (April 1968), pp. 67–74.
5. Li, Tingye, "Diffraction Loss and Selection of Modes in Maser Resonators With Circular Mirrors," B.S.T.J., *44,* No. 5 (May–June 1965), pp. 917–932.
6. Howell, W. T., "On a Class of Function Which are Self Reciprocal in the Hankel Transform," Phil. Mag, *25,* Series 7 (April 1938), pp. 622–628.
7. Erdelyi, A., et. al., *Tables of Integral Transform,* Vol. 2, New York: McGraw-Hill, 1954, p. 43.
8. Boyd, G. D., and Kogelnik, H., "Generalized Confocal Resonator Theory," B.S.T.J., *41,* No. 4 (July 1962), pp. 1347–1369.
9. La Tourette, et. al., "Improved Laser Angular Brightness Through Diffraction Coupling," Appl. Opt., *3,* No. 8 (August 1964), pp. 981–982.
10. Vainshtein, L. A., "Open Resonators for Lasers," Sov. Phys., JETP, *17* (September 1963), pp. 709–719.
11. Buchholz, H., *Die Konfluente Hypergeometrische Function,* Berlin: Springer-Verlag, 1953, p. 144.
12. Gradshteyn, I. S., and Ryzhik, I. M., *Tables of Integrals, Series and Products,* New York: Academic Press, 1965, pp. 845 and 1035.